that does not require calculation of derivatives is to look for random changes (controlled in appropriate ways) in the parameter values that reduce the error. In the simulations described in this report the model was endowed with a dual, incremental learning mechanism. First, when the model's performance on a new input was markedly inadequate (in comparison with recent history), that input was adjoined to the model as an additional center (prototype). This happened mainly in the initial trials, with the number of centers eventually reaching an asymptote that depended on the nature of the task and on the parameters that affected the decision to add new centers. The performance of the model during these first trials improved quickly, then stabilized as the number of centers approached the asymptote. Second, further gradual improvement in the performance was obtained by letting the model carry out a local random search in the space of existing HyperBF center coordinates. This search was guided by feedback given to the model (that is, by indicating whether the response at each trial was correct). Details of the learning algorithms, including an extension of the incremental learning algorithm to a situation in which no explicit feedback is available, can be found in (*6, 7*).

5. A description of multilayer perceptrons and the back-propagation technique used for learning is in D. E. Rumelhart, G. E. Hinton, R. J. Williams, *Nature* **323**, 533 (1986). An overview of some of the classical techniques can be found in S. Omohundro [*Complex Syst.* 1, 273 (1987)] and in R. O. Duda and P. E. Hart [*Pattern Classification and Scene Analysis* (Wiley, New York, 1973)]. Relations between multilayer perceptrons and HyperBF networks are mentioned in (*4*) and studied in M. Maruyama, F. Girosi, T. Poggio, *A.I. Memo No. 1291* (Artificial Intelligence Laboratory, Massachusetts Institute of Technology, Cambridge, MA, 1992).
6. T. Poggio, M. Fahle, S. Edelman, *A.I. Memo No. 1271* (Artificial Intelligence Laboratory, Massachusetts Institute of Technology, Cambridge, MA, 1991); S. Edelman, T. Poggio, M. Fahle, *Comput. Vision Graph. Image Process.* B, in press. The simulation results were robust with respect to all parameters, including the number of inputs.
7. Y. Weiss, S. Edelman, M. Fahle, T. Poggio, *CS-TR 91-21* (Department of Applied Mathematics and Computer Science, Weizmann Institute, Rehovot, Israel, 1991).
8. We have also experimented with a different version of the HyperBF model, in which orientation-selective receptive fields similar to those of simple cells in V1 played the role of the basis functions. See (*7*). This version of the model replicated the absolute values and the time course of the improvement of the thresholds found in human psychophysical data, in addition to replicating the data concerning the percentage of correct responses.
9. Hyperacuity-level performance was independent of the precise location of the receptors. At the same time, different quasi-random receptor mosaics yielded different thresholds, sometimes by as much as a factor of 2. A similar range of hyperacuity thresholds is observed in human subjects, even at full acuity and with perfectly normal eyes.
10. The model also exhibited learning on a longer time scale (*4, 7*), similar to the slow long-term learning component found in human subjects (M. Fahle and S. Edelman, in preparation).
11. R. Watt and F. W. Campbell, *Spat. Vision* 1, 31 (1985).
12. The stimulus in the bisection task consists of three dots, arranged in a vertical line, at an approximately even spacing. The subject has to determine whether the middle dot is above or below the midpoint of the segment formed by the other two dots. The HyperBF module learned this hyperacuity task just as easily as it did in the line vernier case (*6*). Another simulation made a comparison between the line vernier task and a similar one in which each of the line segments has been replaced by two dots (situated at the endpoints). The network learned this task, as it did previously in the line vernier and the bisection cases. The better performance of the HyperBF module in the dot vernier task for small offsets parallels a recent surprising finding with human subjects (M. Fahle, unpublished observations).
13. In a recent study, R. Bennett and G. Westheimer [*Percept. Psychophys.* **49**, 541 (1991)] found surprisingly little learning of thresholds in three-dot alignment and grating discrimination. Their experiments used transfer of training across the stimulus range to probe for learning, hiding possible effects of fast learning that may have happened in the baseline session (p. 544). Interestingly, the lack of transfer across the stimulus range in these experiments is consistent with our notion of experience-based learning.
14. A. Fiorentini and N. Berardi, *Nature* **287**, 43 (1980).
15. A. Karni and D. Sagi, *Proc. Natl. Acad. Sci. U.S.A.* **88**, 4966 (1991).
16. K. Ball and R. Sekuler, *Science* **218**, 697 (1982); S. P. McKee and G. Westheimer, *Percept. Psychophys.* **24**, 258 (1978); V. S. Ramachandran and O. Braddick, *Perception* **2**, 371 (1973).
17. Y. Frégnac, D. Shulz, S. Thorpe, E. Bienenstock, *Nature* **333**, 367 (1988).
18. T. Poggio and S. Edelman, *ibid.* **343**, 263 (1990); S. Edelman and T. Poggio, *Int. J. Pattern Recognit. Artif. Intell.*, in press; S. Edelman and D. Weinshall, *Biol. Cybern.* **64**, 209 (1991).
19. S. Edelman, D. Reisfeld, Y. Yeshurun, *CS-TR 91-20* (Department of Applied Mathematics and Computer Science, Weizmann Institute, Rehovot, Israel, 1991); R. Brunelli and T. Poggio, in *Proceedings of the 12th International Joint Conference on Artificial Intelligence*, International Joint Conference on Artificial Intelligence, Inc., Sydney, Australia, 24 to 30 August 1991 (Kaufmann, Mountain View, CA, 1991); S. Edelman and T. Poggio, *A.I. Memo No. 1181* (Artificial Intelligence Laboratory, Massachusetts Institute of Technology, Cambridge, MA, 1990); R. Brunelli and T. Poggio, *I.R.S.T. TechReport 9110-04* (Instituto per la Ricerca Scientifica e Tecnologica, Trento, Italy, 1991).
20. We are grateful to H. Buelthoff, F. Crick, F. Girosi, R. Held, A. Hurlbert, Y. Weiss, and G. Westheimer for useful discussions and suggestions. Supported by a grant from the Office of Naval Research, Cognitive and Neural Sciences Division, by the Artificial Intelligence Center of Hughes Aircraft Corporation, and by the Deutsche Forschungsgemeinschaft (Heisenberg-Programme). Support for the Artificial Intelligence Laboratory's artificial intelligence research is provided by the Advanced Research Projects Agency of the Department of Defense. T.P. is supported by the Uncas and Helen Whitaker chair.

18 December 1991; accepted 24 March 1991

Synaptotagmin: A Calcium Sensor on the Synaptic Vesicle Surface

Nils Brose,* Alexander G. Petrenko, Thomas C. Südhof, Reinhard Jahn†‡

Neurons release neurotransmitters by calcium-dependent exocytosis of synaptic vesicles. However, the molecular steps transducing the calcium signal into membrane fusion are still an enigma. It is reported here that synaptotagmin, a highly conserved synaptic vesicle protein, binds calcium at physiological concentrations in a complex with negatively charged phospholipids. This binding is specific for calcium and involves the cytoplasmic domain of synaptotagmin. Calcium binding is dependent on the intact oligomeric structure of synaptotagmin (it is abolished by proteclytic cleavage at a single site). These results suggest that synaptotagmin acts as a cooperative calcium receptor in exocytosis.

Calcium-dependent exocytosis of synaptic vesicles is the central step in the sequence of events from the arrival of an action potential to the release of neurotransmitters. It is generally accepted that Ca^{2+} enters the nerve terminal via voltage-gated Ca^{2+} channels in the presynaptic plasma membrane. Intracellular recordings in model synapses such as the squid giant synapse have shown that the latency between Ca^{2+} entry and the release of transmitter is in the range of 200 μs. This implies that a complex between synaptic vesicles and the plasma membrane must exist in the resting state because the time after Ca^{2+} entry is too short to allow for vesicle docking before fusion. Furthermore, the dependence of transmitter release on the intraterminal Ca^{2+} concentration is nonlinear and highly cooperative (*1*).

The Ca^{2+} receptor protein for exocytosis has not been identified. However, certain predictions about its properties can be made. Because of the short latency between Ca^{2+} influx and exocytosis, it is likely that the Ca^{2+} receptor is part of the complex formed between the plasma membrane and the synaptic vesicle and is probably located on one of these membrane compartments. In addition, Ca^{2+} must induce a change in the properties of the receptor protein, which ultimately causes a rearrangement of

N. Brose and R. Jahn, Department of Neurochemistry, Max-Planck-Institute for Psychiatry, D-8033 Martinsried, Germany.
A. G. Petrenko and T. C. Südhof, Howard Hughes Medical Institute and Department of Molecular Genetics, University of Texas Southwestern Medical Center, Dallas, TX 75235.

*Present address: Salk Institute, Molecular Neurobiology Laboratory, 10010 North Torrey Pines Road, La Jolla, CA 92037.
†Present address: Howard Hughes Medical Institute and Department of Pharmacology, Yale University School of Medicine, New Haven, CT 06536.
‡To whom correspondence should be addressed.

phospholipid microdomains at the contact site between the two membranes, leading to membrane fusion. It is unclear how many proteins participate in this process. However, the speed of the event makes it unlikely that major protein rearrangements, such as Ca^{2+}-induced docking of cytosolic proteins, are involved (*1*).

In this report, we present evidence that the synaptic vesicle protein synaptotagmin (also referred to as p65) exhibits properties expected of the exocytotic Ca^{2+} receptor. Synaptotagmin is represented by a family of related integral membrane proteins with widespread distribution (*2–4*). It is specifically localized in the membrane of synaptic vesicles and that of secretory granules in endocrine cells (*2*). Structural analysis of this protein family revealed the existence of two copies of an internal repeat that are homologous to corresponding domains in protein kinase C (C_2 domain) (*3, 4*), in a cytosolic form of phospholipase A_2, and, although with less identity, in guanosine triphosphatase–activating protein and phospholipase C (*5*). In protein kinase C and phospholipase A_2, this domain is thought to be responsible for the Ca^{2+}-dependent binding of these proteins to phospholipid membranes (*5*). This prompted us to investigate whether native synaptotagmin functions as a Ca^{2+} binding protein and whether Ca^{2+} binding by synaptotagmin involves interactions with membrane phospholipids.

To study the properties of synaptotagmin, we isolated the protein from Triton X-100 extracts of rat brain by affinity chromatography, using a newly generated monoclonal antibody (clone Cl 41.1) directed against synaptotagmin I as affinity ligand (*6*). Synaptotagmin I was purified in a single step, resulting in a protein of more than 90% purity.

We studied the Ca^{2+} binding to purified synaptotagmin by equilibrium dialysis either in the presence or in the absence of phospholipids (*7*). As controls, Ca^{2+} binding to phospholipids alone or to purified synaptophysin, an integral membrane protein of synaptic vesicles (*8*), was monitored under identical experimental conditions. No Ca^{2+} binding to synaptotagmin was observed in the absence of phospholipids (Fig. 1). However, when liposomes containing 25% phosphatidylserine and 75% phosphatidylcholine were added, a dramatic increase in Ca^{2+} binding over that of the phospholipid control was observed (Fig. 1). The Ca^{2+} binding reached 4 mol per mole of synaptotagmin subunit at a free Ca^{2+}

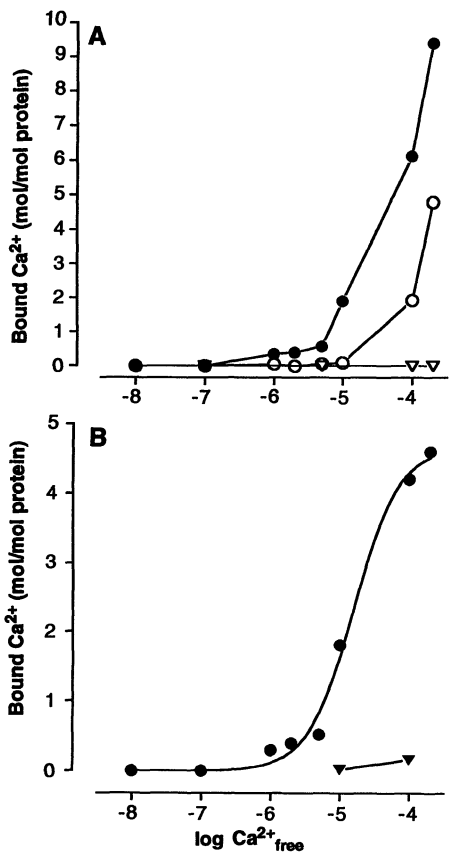

Fig. 1. Binding of Ca^{2+} to synaptotagmin in the presence or absence of phospholipid vesicles, determined by equilibrium dialysis (*7*). As control, Ca^{2+} binding to protein-free liposomes is shown. (**A**) Total Ca^{2+} binding: (●) synaptotagmin plus phospholipid vesicles; (○) phospholipid vesicles alone; (▽) synaptotagmin alone. Note that phospholipid vesicles bind Ca^{2+} in a linear dependence on the Ca^{2+} concentration. (**B**) Net Ca^{2+} binding to synaptotagmin (●) and, as control, to synaptophysin (▼), in the presence of phospholipids. We obtained the values by subtracting binding to phospholipids alone from total binding. Numbers of moles were calculated on the basis of the molecular weight of the monomers, respectively.

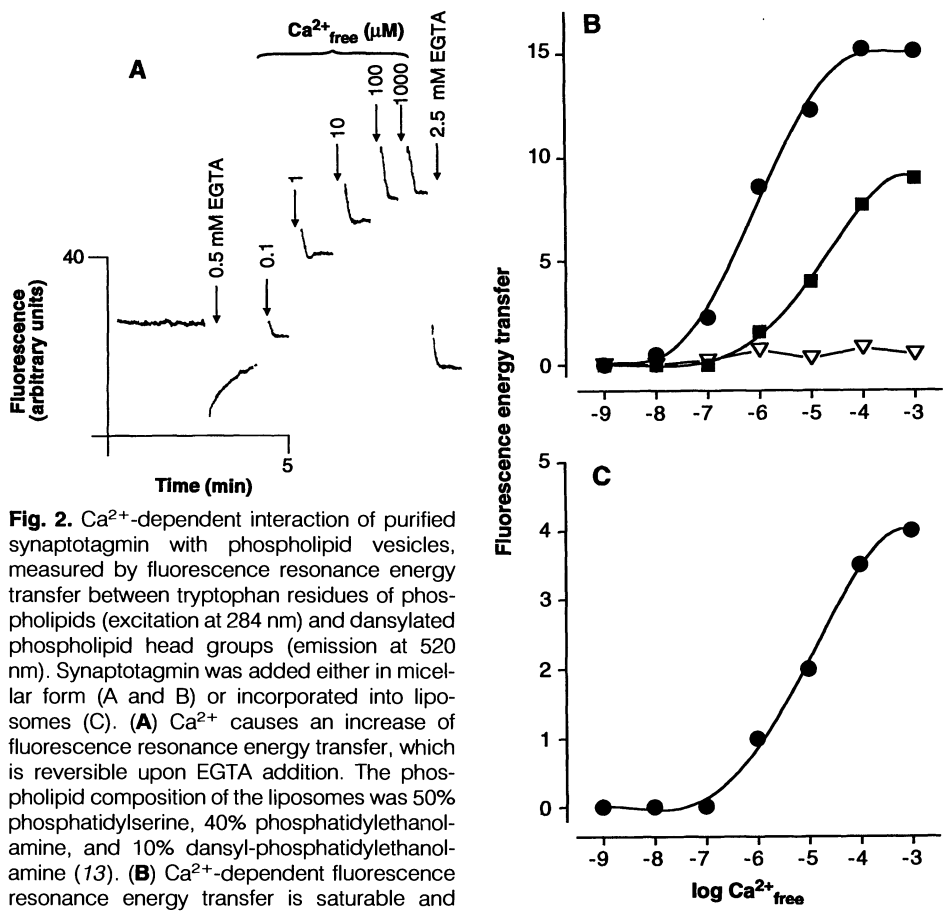

Fig. 2. Ca^{2+}-dependent interaction of purified synaptotagmin with phospholipid vesicles, measured by fluorescence resonance energy transfer between tryptophan residues of phospholipids (excitation at 284 nm) and dansylated phospholipid head groups (emission at 520 nm). Synaptotagmin was added either in micellar form (A and B) or incorporated into liposomes (C). (**A**) Ca^{2+} causes an increase of fluorescence resonance energy transfer, which is reversible upon EGTA addition. The phospholipid composition of the liposomes was 50% phosphatidylserine, 40% phosphatidylethanolamine, and 10% dansyl-phosphatidylethanolamine (*13*). (**B**) Ca^{2+}-dependent fluorescence resonance energy transfer is saturable and depends on the phospholipid composition. Values were expressed as a percentage change in emission intensity, $I_{net} = (I - I_0) \times 100/I_0$, where I is the recorded fluorescence intensity in the experiment and I_0 is the reference fluorescence intensity in the absence of Ca^{2+}. (●) Liposomes containing 50% phosphatidylserine, 40% phosphatidylethanolamine, and 10% dansyl-phosphatidylethanolamine (mean values of three independent experiments); (■) liposomes containing 25% phosphatidylserine, 65% phosphatidylethanolamine, and 10% dansyl-phosphatidylethanolamine; (▽) control, using an assay mixture as in (●) that was digested for 1 hour at 37°C with trypsin (1 μg/ml) before the experiment (*14*) (data shown are from a representative experiment). (**C**) Ca^{2+}-dependent fluorescence resonance energy transfer between synaptotagmin-containing donor liposomes and dansylated acceptor liposomes. The donor liposomes were composed of 45% phosphatidylcholine, 45% phosphatidylethanolamine, and 10% phosphatidylserine; the acceptor liposomes were the same as in (A).

concentration of 10^{-4} M (Fig. 1). In contrast, no significant Ca^{2+} binding was observed up to a concentration of 10^{-4} M when purified synaptophysin instead of synaptotagmin was used, regardless of whether phospholipids were present (Fig. 1). This indicates that, contrary to an earlier report (8), synaptophysin does not bind Ca^{2+}. Thus, the ability to bind Ca^{2+} is a specific, intrinsic property of synaptotagmin.

To study the interaction between synaptotagmin and phospholipids in more detail, we utilized a fluorescence resonance energy transfer assay. Dansyl-phosphatidylethanolamine was incorporated into liposomes. These liposomes were mixed with purified synaptotagmin. Fluorescence resonance energy transfer between tryptophan residues in synaptotagmin and the dansyl group in the liposomes was measured as a function of Ca^{2+}. Energy transfer is highly dependent on the distance between the two fluorophores and is only observed on close contact of the protein and the lipid fluorescent probe. We found that Ca^{2+} triggered fluorescence resonance energy transfer in a dose-dependent manner (Fig. 2A), suggesting that Ca^{2+} causes a close association of synaptotagmin with the dansyl liposomes. The signals were reversed by addition of EGTA (Fig. 2A) and reestablished by subsequent addition of excess Ca^{2+} (not shown), demonstrating that the interaction is reversible. Liposomes alone showed no change in fluorescence on addition of Ca^{2+}. Furthermore, no energy transfer was observed up to a Ca^{2+} concentration of 1 mM when synaptotagmin was subjected to mild proteolysis with trypsin before the experiment (Fig. 2B) or when equal amounts of purified synaptophysin or purified immunoglobulin G (IgG) were used instead of synaptotagmin (not shown). These controls demonstrate that this assay measures the specific Ca^{2+}-dependent interaction of synaptotagmin with liposomes.

Energy transfer between synaptotagmin and liposomes was specific for Ca^{2+} (Mg^{2+}, Ba^{2+}, or Sr^{2+} did not evoke a response at concentrations up to 1 mM; these metal ions were also unable to interfere with the Ca^{2+} signal). However, an increase in both the Ca^{2+} sensitivity and the intensity of the signal was observed when the proportion of phosphatidylserine in the acceptor liposomes was increased to 50% (Fig. 2B). This indicates that the acidic head groups may participate directly in the formation of the synaptotagmin-Ca^{2+}-phospholipid complex, which is in agreement with the previously determined phospholipid binding specificity of recombinant synaptotagmin (3).

For a given phospholipid composition (25% acidic phospholipids), the dependence of phospholipid binding on the Ca^{2+} concentration was remarkably similar to that of Ca^{2+} binding measured by equilibrium dialysis, with a half-maximal response at 10^{-5} M Ca^{2+} (compare Figs. 1B and 2B). Although the precise phospholipid composition of the presynaptic plasma membrane is not known, a proportion of 25% acidic phospholipids is probably a low estimate. Because an increase in acidic phospholipid content drastically shifts the Ca^{2+} sensitivity to lower concentrations, the response lies well within the Ca^{2+} concentration range expected upon excitation at the contact site between synaptic vesicles and the plasma membrane.

To ensure that synaptotagmin can also interact with phospholipid vesicles when the protein itself is incorporated in a phospholipid vesicle, we purified the protein from cholate extracts and reconstituted it into liposomes by a dialysis procedure. When acceptor liposomes containing dansylated head groups were added to these liposomes, Ca^{2+}-dependent fluorescence resonance energy transfer was observed, which was similar to that observed with the purified protein alone (Fig. 2C). As an independent confirmation for Ca^{2+}-depen-

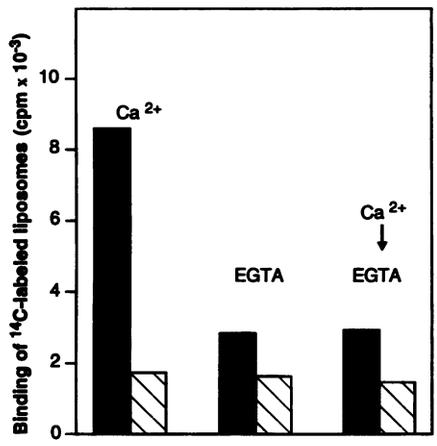

Fig. 3. Radiolabeled liposomes bind reversibly to synaptotagmin immobilized to protein G–Sepharose. Purified synaptotagmin (10 μg), suspended in 50 μl of 20 mM tris-Cl (pH 7.2), 100 mM NaCl was incubated with 20 μg of purified monoclonal antibody to synaptotagmin for 1 hour at 4°C and bound to protein G–Sepharose by further incubation for 1 hour (8-μl bed volume). Additions of Ca^{2+} (left pair of bars) or EGTA (middle pair of bars) were made to give final concentrations of 1 mM. Binding was started by the addition of 100 μl (500 μg) of ^{14}C-labeled liposomes, prepared from 50% phosphatidylserine and 50% phosphatidylethanolamine, and carried out for 10 min. To some Ca^{2+}-containing samples, EGTA was then added to give a final concentration of 1.5 mM and the incubation was continued for 5 min (right pair of bars). The reaction was stopped by removal of the assay mixture from the beads by filtration. The beads were rapidly washed twice with incubation buffer containing 1 mM Ca^{2+} (left pair of bars) or 1 mM EGTA (middle and right pairs of bars) and analyzed by liquid scintillation counting. Hatched bars show background binding of liposomes to protein G–Sepharose containing monoclonal antibody but no synaptotagmin.

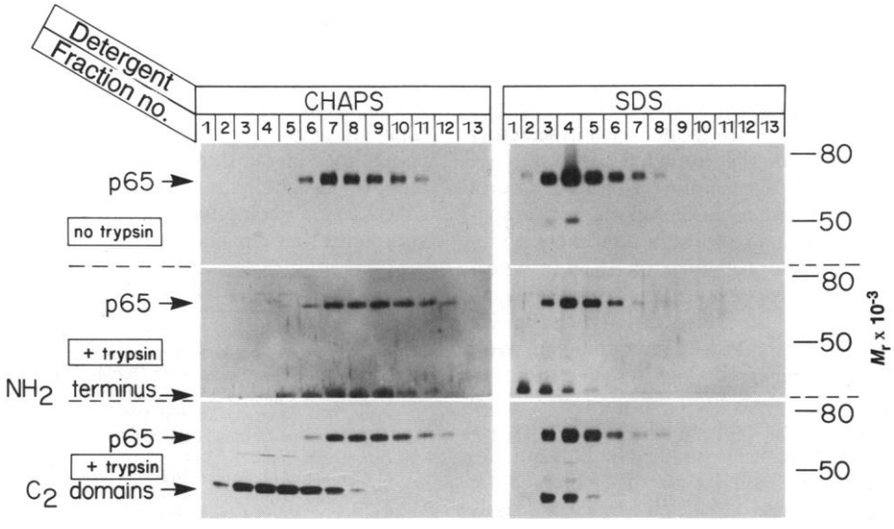

Fig. 4. Mild proteolytic cleavage of synaptotagmin results in monomeric fragments containing the C_2 domains and oligomeric NH_2-terminal fragments. Intact synaptotagmin (p65) or synaptotagmin cleaved at a single site by low doses of trypsin was solubilized from synaptic vesicles, and its apparent size (M_r) was analyzed by sucrose gradient centrifugation in the presence of CHAPS (left) or SDS (right). Fractions were immunoblotted after SDS-PAGE with an antibody either to the C_2 domains or to the NH_2-terminus of synaptotagmin, and immunoreactive bands were visualized with chemoluminescence. Analysis of fractions in cholate or octylglucoside as detergents gave results similar to those in CHAPS (not shown) (15).

dent interaction of synaptotagmin with phospholipid vesicles, we measured the binding of radiolabeled liposomes to immobilized synaptotagmin. Whereas in the presence of EGTA a small but significant amount of phospholipid binding was observed, Ca^{2+} induced a four- to sixfold increase over the basal binding, which was abolished upon subsequent addition of EGTA (Fig. 3).

In synaptic vesicles, synaptotagmin is present as a homo-oligomeric complex of probably four subunits containing eight C_2 domains (9). To evaluate whether Ca^{2+}-phospholipid binding by synaptotagmin is dependent on an intact oligomeric structure, we subjected the protein to limited proteolysis. Under these conditions, cleavage occurs at a single site adjacent to the membrane spanning domain, creating a large cytoplasmic fragment that contains both C_2 domains (3). This cleavage abolished the ability of synaptotagmin to bind Ca^{2+} or phospholipids in a Ca^{2+}-dependent manner as measured with the assays described above (Fig. 2B). To analyze the structure of the proteolytic fragments in more detail, we determined their size by sucrose density gradient centrifugation in CHAPS. For comparison, the migration of the fragments was monitored in SDS, which dissociates all aggregates into monomers. The NH_2-terminal fragment of synaptotagmin comigrates with uncleaved synaptotagmin in a high molecular weight complex (Fig. 4), clearly separated from the larger COOH-terminal fragment, which migrates at a monomer position. These results suggest that tetramerization of synaptotagmin, mediated by its NH_2-terminal domain, is required for formation of the complex with Ca^{2+} and phospholipids.

Synaptotagmin is the first Ca^{2+}-binding protein that has been identified in secretory organelles of the regulated pathway. The widespread distribution of at least one of the synaptotagmin isoforms on every synaptic vesicle and probably also every endocrine secretory granule (2–4) is in agreement with a general role as putative Ca^{2+} receptor for exocytosis. The precise nature of the interaction of synaptotagmin with phospholipids and Ca^{2+} remains to be established. Synaptotagmin, Ca^{2+}, and membrane phospholipids probably form a ternary complex or sandwich. This interdependence is similar to that observed for protein kinase C, which binds Ca^{2+} only when phospholipids are present (10). In the absence of Ca^{2+}, some phospholipid binding was observed (Fig. 3). This is in agreement with our earlier observation that the recombinant cytoplasmic fragment of synaptotagmin is capable of Ca^{2+}-independent phospholipid binding after being subjected to denaturing SDS-polyacrylamide gel electrophoresis (SDS-PAGE) and immunoblotting (3).

Because Ca^{2+}-phospholipid binding was abolished by proteolytic cleavage at a single site, the responsibility of the C_2 domains could not be unambiguously established although it seems likely in analogy to protein kinase C and phospholipase A_2. The observation of fluorescence resonance energy transfer between tryptophan and phospholipids strongly supports an involvement of the C_2 domains because these domains contain the only tryptophan residues of the entire structure, the single exception being a tryptophan residue located in the membrane-spanning domain, which is unlikely to be included. However, the results indicate that an intact tetrameric structure of the protein is required for Ca^{2+} binding. This requirement and the presence of multiple Ca^{2+}-binding sites may explain the high cooperativity observed for Ca^{2+} in triggering transmitter release.

How does synaptotagmin function in exocytosis? Although we have demonstrated Ca^{2+}-dependent binding of synaptotagmin-containing membrane vesicles to acceptor liposomes, we do not believe that this property is solely responsible for vesicle docking to the presynaptic plasma membrane. Instead, we assume that in the resting nerve terminal where the Ca^{2+} concentration is low (1), synaptotagmin forms a complex with a specific acceptor protein in the plasma membrane. We have recently reported that synaptotagmin binds specifically to the α-latrotoxin receptor in vitro (11), suggesting that this protein serves as the vesicle docking protein in the presynaptic membrane. When such a docking complex is exposed to increased Ca^{2+} concentrations, it probably results in an interaction of the cytoplasmic arms of synaptotagmin with the phospholipids of the plasma membrane, causing local rearrangement of phospholipids (12). This may then trigger fusion via interaction with additional proteins that remain to be characterized.

REFERENCES AND NOTES

1. R. Llinas, I. Z. Steinberg, K. Walton, *Biophys. J.* **33**, 289 (1981). For a review, see also L. Reichardt and R. B. Kelly, *Annu. Rev. Biochem.* **52**, 871 (1983); G. Augustine, M. P. Charlton, S. J. Smith, *Annu. Rev. Neurosci.* **10**, 633 (1987).
2. W. E. Matthew, L. Tsavaler, L. F. Reichardt, *J. Cell. Biol.* **91**, 257 (1981).
3. M. S. Perin *et al.*, *Nature* **343**, 260 (1990); *J. Biol. Chem.* **266**, 615 (1991); M. S. Perin, N. Brose, R. Jahn, T. C. Südhof, *ibid.*, p. 623.
4. M. Geppert, B. T. Archer III, T. C. Südhof, *ibid.*, p. 13548; B. Wendland *et al.*, *Neuron* **6**, 993 (1991).
5. J. D. Clark *et al.*, *Cell* **65**, 1043 (1991). For a review, see also Y. Nishizuka, *Nature* **334**, 661 (1988).
6. The monoclonal antibody was generated by standard procedures [G. Köhler and C. Milstein, *Nature* **256**, 495 (1975); R. Jahn, W. Schiebler, C. Ouimet, P. Greengard, *Proc. Natl. Acad. Sci. U.S.A.* **82**, 4137 (1985)] with recombinant synaptotagmin (3) used as antigen. Preparation of the affinity matrix (1-ml final volume, containing ~8 mg of purified IgG) and purification of synaptotagmin (and synaptophysin) were performed essentially as described earlier for synaptophysin [F. Navone *et al.*, *J. Cell Biol.* **103**, 2511 (1986)], by using a Triton X-100 extract of rat brain membranes as starting material. Protein was eluted in 0.05% Triton X-100 and dialyzed for 2 days against six buffer changes before the experiments. Yields were between 0.2 and 0.4 mg of protein per preparation.
7. Ca^{2+} binding was measured with an equilibrium dialysis assay (10). Dialysis samples contained 0.2 to 0.6 mg of protein (synaptotagmin or synaptophysin) per milliliter or 1.7 mg of phospholipid vesicles (75% phosphatidylcholine, 25% phosphatidylserine) per milliliter, which were prepared as described in (13). As an internal standard to follow sample dilution during dialysis, liposomes containing ^3H-labeled phosphatidylcholine (6 μCi/mg), which do not bind synaptotagmin or synaptophysin, were added to a final concentration of 0.33 mg/ml. Concentrations of free Ca^{2+} were adjusted in an EGTA-Ca^{2+} buffer system. We calculated the EGTA and Ca^{2+} concentrations needed to give the desired free Ca^{2+} concentrations using computer software developed by K. J. Föhr, W. Warhol, and M. Gratzl (*Methods Enzymol.*, in press). Samples were dialyzed for 12 hours against large volumes of [^{45}Ca]Ca^{2+} containing buffer and then assayed for ^{45}Ca and ^3H by scintillation counting.
8. H. Rehm, B. Wiedenmann, H. Betz, *EMBO J.* **5**, 535 (1986). For a review on synaptophysin and other synaptic vesicle proteins, see also T. C. Südhof and R. Jahn, *Neuron* **6**, 665 (1991).
9. Evidence that synaptotagmin is a tetramer: Using a variety of detergents, we found that synaptotagmin migrates at a similar position on sucrose gradients. This position is different from that of synaptophysin, synaptobrevin, synapsin, synaptoporin, and the proton pump, suggesting that synaptotagmin is not part of an artifactual high molecular weight complex due to insufficient solubilization (3). In the presence of Zwittergent 3-14, synaptotagmin migrates at a dimer position. This is surprising because in the inositol trisphosphate receptor, Zwittergent 3-14 disrupts interactions between transmembrane regions totally [G. A. Mignery, C. L. Newton, B. T. Archer, T. C. Südhof, *J. Biol. Chem.* **265**, 12679 (1990)]. Because dimers can also be observed in SDS-PAGE, we think that two strongly bonded dimers form a tetramer.
10. M. D. Bazzi and G. L. Nelsestuen, *Biochemistry* **29**, 7624 (1990).
11. A. G. Petrenko *et al.*, *Nature* **353**, 65 (1991).
12. Such lateral rearrangement of phospholipids has been demonstrated for protein kinase C (where association of the protein with membranes in the presence of Ca^{2+} leads to extensive segregation of acidic phospholipids [M. D. Bazzi and G. L. Nelsestuen, *Biochemistry* **30**, 7961 (1991)] and for various other proteins and polycations [W. Hartmann and H. J. Galla, *Biochim. Biophys. Acta* **509**, 474 (1978); D. Carrier and M. Pezolet, *Biochemistry* **25**, 4167 (1986); G. B. Birrel and O. H. Griffith, *ibid.* **15**, 2925 (1976); J. M. Boggs *et al.*, *ibid.* **15**, 5420 (1976); T. Ikeda *et al.*, *Biochim. Biophys. Acta* **1026**, 105 (1990)]. Furthermore, Ca^{2+}-dependent binding of synaptotagmin to calmodulin was reported [J. M. Trifaro, S. Fournier, M. L. Novas, *Neuroscience* **29**, 1 (1989)], which, however, could not be reproduced in our laboratories.
13. Liposomes were prepared from purified phospholipids (Avanti Polar Lipids) dissolved in chloroform:methanol, 9:1). The solvent was evaporated under a stream of nitrogen and then further dried under vacuum for 30 min. Then 20 mM tris-Cl (pH 7.2) and 100 mM NaCl were added to give a final phospholipid concentration of 0.2 mg/ml. Phospholipids were resuspended by vigorous vortexing (glass beads). Liposomes were formed by ultrasonication in a Branson bath-sonicator for 5

min at maximal power output. The opalescent emulsion was centrifuged for 20 min at 20,000*g* to remove aggregated material. Fluorescence resonance energy transfer assays were performed as described (*10*). In Fig. 2, A and B, 40 μg of purified synaptotagmin or synaptophysin were incubated with 10 μg of liposomes in 1 ml of 20 mM tris-Cl (pH 7.2), 100 mM NaCl, 0.5 mM EGTA. The free Ca^{2+} concentration was increased by successive additions of 20 mM or 100 mM solutions of $CaCl_2$ to give the free Ca^{2+} concentrations indicated. In Fig. 2C, synaptotagmin was purified from a membrane extract prepared in 1% sodium cholate instead of Triton X-100, dialyzed against 20 mM tris-Cl (pH 7.2), 100 mM NaCl, 1% sodium cholate, 2 mM phenylmethylsulfonyl fluoride, and Pepstatin A (1 μg/ml) and combined with 60 μg of phospholipids per 100 μg of synaptotagmin resuspended in the same buffer (10% phosphatidylserine, 45% phosphatidylcholine, 45% phosphatidylethanolamine). Liposomes were formed by dialysis against cholate-free buffer.

14. In all proteolysis experiments, the degree of proteolysis was monitored by SDS-PAGE, followed by fragment visualization with site-specific antibodies (*3*). Conditions were chosen in which all synaptotagmin was cleaved but only minor further degradation of the fragments had occurred.
15. In the sucrose gradient centrifugations crude synaptic vesicles were solubilized with 1% (w/v) SDS or 2% (w/v) CHAPS, cholate, or β-octylglucoside in 75 mM tris-Cl (pH 7.4), 1 mM EDTA. Solubilized proteins were loaded on 11.8 ml of 5 to 20% (w/v) sucrose gradients containing 0.1% of the respective detergent in the same buffer as above. For SDS-solubilized proteins, 350 μg of total protein were loaded in a 100-μl volume; for all other detergents, 260 μg of total protein were loaded in a 300-μl volume. Gradients were centrifuged for 16 hours at 4°C at 38,000 rpm in a Beckman SW41 rotor and fractionated into 24 0.5-ml fractions. For the experiments utilizing partially trypsinized synaptotagmin, synaptic vesicles were incubated with trypsin in a protein mass ratio of 1:6000 before solubilization, and samples were solubilized in CHAPS or SDS. On parallel gradients, the positions of molecular size markers were as follows: carbonic anhydrase (29 kD), fractions 2 and 3; bovine serum albumin (67 kD), fraction 4; alcohol dehydrogenase (155 kD), fraction 6; β-amylase (200 kD), fraction 8; apoferritin (443 kD), fractions 14 and 15. We analyzed fractions by SDS-PAGE and immunoblotting, using the Amersham enhanced chemiluminescence system according to the manufacturer's directions with polyclonal antibodies to the NH_2-terminus and the C_2 domains of synaptotagmin as described (*3*).
16. We thank M. D. Bazzi for advice concerning the Ca^{2+} equilibrium dialysis and fluorescence resonance energy transfer experiments, H. Schauerte and S. Schieback for help in some of the experiments, and P. R. Maycox for critical reading of the manuscript.

23 December 1991; accepted 9 March 1992

High-Frequency Network Oscillation in the Hippocampus

György Buzsáki,* Zsolt Horváth, Ronald Urioste, Jamille Hetke, Kensall Wise

Pyramidal cells in the CA1 hippocampal region displayed transient network oscillations (200 hertz) during behavioral immobility, consummatory behaviors, and slow-wave sleep. Simultaneous, multisite recordings revealed temporal and spatial coherence of neuronal activity during population oscillations. Participating pyramidal cells discharged at a rate lower than the frequency of the population oscillation, and their action potentials were phase locked to the negative phase of the simultaneously recorded oscillatory field potentials. In contrast, interneurons discharged at population frequency during the field oscillations. Thus, synchronous output of cooperating CA1 pyramidal cells may serve to induce synaptic enhancement in target structures of the hippocampus.

Much of what is known about the physiological function of the hippocampus is based on in vivo and in vitro studies of sequentially analyzed single neurons (*1*, *2*). Although it has long been believed that the computational power of complex neuronal networks cannot be recognized by the properties of single cells alone (*3*), experimental access to the emergent properties of cooperating hippocampal neurons has been difficult. Direct investigation of the time-varying organization of neuronal populations requires the simultaneous observation of many individual neurons in the awake animal (*4*). Using silicon multichannel recording arrays (*5*), we report here the physiological details of a high-frequency oscillation of the hippocampal CA1 neuronal network that is a specific product of cellular cooperativity.

The data analyzed in this study were recorded from 19 adult male rats. Local field potentials and unit activity were recorded by multichannel microprobes (*5*, *6*) in the rat during spontaneous behaviors and sleep (*7*). The oscillatory behavior of the recorded cell populations and local field potentials was determined by the periodic modulation of the auto- and cross-correlograms (*8*).

Local field potentials in the CA1 strata pyramidale and radiatum were related to cellular firing during awake immobility (Fig. 1). Sharp waves in the stratum radiatum of the CA1 network reflect depolarization of the apical dendrites of pyramidal cells by the Schaffer collaterals, which is a result of the synchronous bursting of CA3 pyramidal cells (*9*, *10*). In conjunction with the stratum radiatum sharp waves, fast field oscillations were present in the CA1 pyramidal layer (*1*, *9*, *10*). The spindle-shaped oscillatory pattern consisted of 5 to 15 sinusoid waves with 200-Hz intraburst frequency. Neuronal discharges most often occurred during the local field oscillations. Isolated pyramidal cells usually fired a single action potential during the field oscillations but occasionally fired a burst of two to three spikes (*11*). The probability of spike bursts (complex spikes) was three to eight times higher during the fast field oscillations than during comparable time periods in their absence.

The laminar distribution of the fast field oscillations was determined by advancing linear arrays of electrodes (*6*) perpendicular to the CA1 pyramidal layer. Amplitude maxima of the fast field oscillations were found in the pyramidal layer (0.2 to 1 mV), and the polarity of the signal reversed in phase about 100 μm below the pyramidal layer, which suggests that the main current source of the extracellularly recorded fast field oscillations is the cell bodies of pyramidal cells.

Typically, less than 15% of the recorded neurons were active during a single oscillatory epoch. When discharges of all neurons

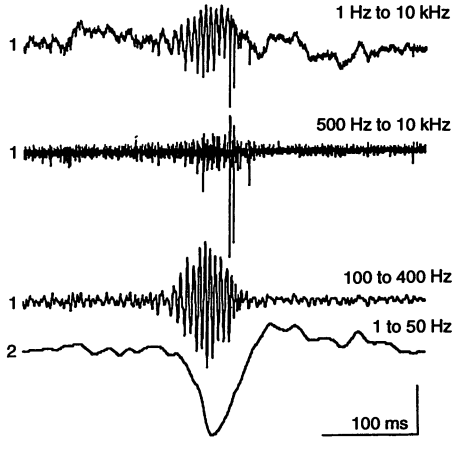

Fig. 1. Fast field oscillation in the CA1 region of the dorsal hippocampus. Simultaneous recordings from the CA1 pyramidal layer (electrode 1) and stratum radiatum (electrode 2). Uppermost trace of electrode 1 is wide-band recording (1 Hz to 10 kHz). Second and third traces are digitally filtered derivatives of the wide-band trace (unit activity 500 Hz to 10 kHz and fast field oscillation (100 to 400 Hz). Note simultaneous occurrence of fast field oscillations, unit discharges, and sharp wave (electrode 2). Electrode 2 was 200 μm below the pyramidal layer. Calibrations: 0.5 mV (trace 1), 0.25 mV (traces 2 and 3), and 1.0 mV (trace 4).

G. Buzsáki, Z. Horváth, R. Urioste, Center for Molecular and Behavioral Neuroscience, Rutgers University, 197 University Avenue, Newark, NJ 07102.
J. Hetke and K. Wise, Center for Integrated Sensors and Circuits, University of Michigan, Ann Arbor, MI 48109.

*To whom correspondence should be addressed.